JOURNAL OF THE ROYAL SOCIETY Interface

O_2 microsensors for minimally invasive tissue monitoring

W. Wang and P. Vadgama

J. R. Soc. Interface 2004 **1**, 109-117
doi: 10.1098/rsif.2004.0013

THE ROYAL SOCIETY

J. R. Soc. Interface (2004) **1**, 109–117
DOI: 10.1098/rsif.2004.0013

O_2 microsensors for minimally invasive tissue monitoring

W. Wang[1] and P. Vadgama[2,†]

[1] *Medical Engineering Division, Department of Engineering, Mile End Road, Queen Mary, University of London, London E1 4NS, UK*
[2] *Interdisciplinary Research Centre in Biomedical Materials, Mile End Road, Queen Mary, University of London, London E1 4NS, UK*

Tissue oxygenation is a key factor ensuring normal tissue functions and viability. Continuous real-time monitoring of the partial pressure of oxygen, pO_2, in tissues gives insight into the dynamic fluctuations of O_2 supplies to tissues by blood circulation. Small oxygen sensors enable investigations of the spatial variation of pO_2 in tissues at different locations in relation to local microvessels. In this paper, pO_2 measurement using microelectrodes and biocompatible sensors is discussed and recent progress of their application in human skin is reviewed. Emphasis is given to working principles of a number of existing oxygen sensors and their potential application *in vivo* and in tissue engineering. Results on spatial and temporal variations of the pO_2 in human skin introduced by localized ischaemia-reperfusion are presented when the surface of the skin is covered by an oxygen-free paraffin oil layer and the range of the tissue pO_2 is deduced to be between 0 and 60 mmHg. In the study, pO_2 increases from 8.0 ± 3.2 mmHg ($n = 6$) at the surface of the skin to 35.2 ± 8.0 mmHg ($n = 9$) at a depth just above the sub-papillary plexus. Temporal decay in pO_2 following tissue compression and rise in pO_2 following pressure release can be described using mono-exponential functions. The time constant for the exponential decay, $\tau = 8.44 \pm 1.53$ s ($n = 7$) is consistently greater than that for the exponential rises, $\tau' = 4.75 \pm 0.82$ s ($n = 6$). The difference in pO_2 change with the time following tissue compression and pressure release reveals different dynamic mechanisms involved in the two transient phases. The elevated steady state pO_2 following reperfusion, which is approximately 20% higher than the pre-occlusion value, indicates localized reactive hyperaemia. Possible applications of O_2 microsensors in diseases, e.g. tumours, pressure ulcers, are also discussed.

Keywords: microelectrode; biocompatible sensors; tissue oxygen partial pressure

1. BACKGROUND

The capability to monitor O_2 on a continuous real-time basis gives the opportunity to both assess dynamic fluctuations, and to make a predictive assessment of O_2 trends in any particular localized environment. Electrochemical and optical (fibre-optic) sensors provide a near-ideal means of localized tissue monitoring other than totally non-invasive methods such as the near-infrared monitoring of the inter-converting Hb/HbO_2 chromophore pair pioneered by Jöbsis (1977). In both electrochemical and optical sensors, a direct interfacial reaction takes place, which can be conveniently amplified and translated into a continuous electrical output using systems suitable for near-patient use. A key capability is that of virtually reagentless measurement in an optically opaque tissue matrix—ideal for subcutaneous measurement. With the advent of miniaturization techniques, including those adapted from the microelectronics industry, ethically acceptable, clinically invasive monitoring becomes feasible.

Application criteria include sensitivity, selectivity, stability, biocompatibility, reliability and overall safety. Undoubtedly, an important route to overcoming many of these problems was to retain sensors behind permselective membranes and appropriate encapsulants (McDonnell & Vadgama 1989). Interfacing with appropriate polymer membrane coverings has permitted the operation of many sensors independently of solution variables presented by the *in vivo* milieu.

2. ELECTROCHEMICAL O_2 MONITORING

The polarographic principle of electrochemical O_2 reduction at a noble metal polarized at approximately -0.65 V versus Ag/AgCl has often been used to produce working oxygen electrodes. However, in the Clark electrode design (Clark 1956), O_2 permeable membrane separates an entire (two electrode) electrochemical cell from the unmodified, undiluted biological matrix. This methodology has been the mainstay of implantable O_2 sensors. The membrane, typically of PTFE, has a crucial role in restricting O_2 permeability sufficiently to limit evolved diffusion gradients to within the physical

† Author for correspondence (p.vadgama@qmul.ac.uk).

Received 24 June 2004
Accepted 28 September 2004
Published online 18 October 2004

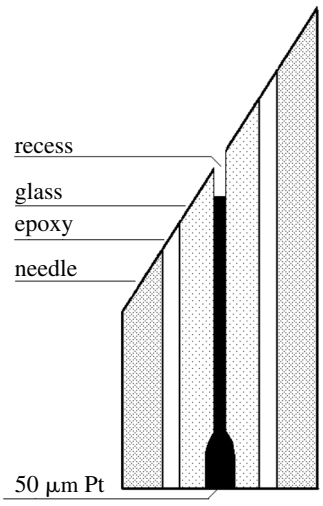

Figure 1. Polarographic 'stab' electrode for tissue pO_2 monitoring (after van der Kleij & de Koning 1981).

confines of the membrane material itself, so avoiding further impact of sample O_2 permeability variation due to sample matrix alteration—a particular consideration when devices are implanted within tissue.

For tissue monitoring such probes have needed to be of reduced diameter, and have tended to be fragile and difficult to construct. In early studies, van der Kleij & de Koning (1981) constructed a needle electrode (figure 1) utilizing a platinum wire cathode of 5 μm diameter insulated in glass, and incorporated into a spinal needle of 0.5 mm bore. Here, to avoid a separate reference electrode, stainless steel was used as the anode (Whalen & Spande 1980). The key feature of this electrode is that the working electrode is protected and O_2 diffusion gradients are internalized within the fluid column of the recess so that, as with a low permeability covering membrane, the diffusion field extending into the tissue matrix is negligible, and so sample matrix independent O_2 flux to the working electrode results which therefore only reflects local pO_2. Schneiderman & Goldstick (1978) examined the influence of recess dimensions and aspect ratios to determine the influence of externalized diffusion fields around the electrode tip. Undoubtedly, a recessed tip structure is able to stabilize O_2 measurements and to some extent protect the working electrode surface from biofouling. Indeed, Davies & Brink (1942) had previously concluded that recessed tip electrodes and intermittent voltage pulses to the working electrode were the only means of obtaining reliable pO_2 measurements in tissue.

Tissue pO_2 relates to the oxygen concentration through the solubility of the oxygen in the tissue, i.e. tissue oxygen partial pressure is equal to the solubility coefficient of the oxygen in the tissue times the concentration of the dissolved oxygen. Interest in tissue pO_2 has increased in view of the radiosensitization of O_2 and the value of relating oxygen tension to radiation dose. There was also the realization that steep O_2 gradients exist in tissue, and that it was necessary to understand the three-dimensional profile of pO_2, particularly in relation to the microcirculation. The additional advantage of using a microelectrode is the limit to the competition for O_2 consumption with cells in the immediate environment of the device. Silver (1987) discussed the relevant issues, and concluded that intermittent sweep potentials applied to the working electrodes reduced O_2 consumption and minimized equilibration time, thereby reducing artefactual influences on tissue and facilitating rapid clinical measurement. With the advent of microfabrication, miniaturized planar O_2 electrodes have been produced. In one example, Suzuki *et al.* (1990) produced a 350 μm deep silicon structure with anisotropically etched v-grooves, which contained electrolytes and the surfaces of which included a cathode (working electrode) and an anode. This internal micro-reaction chamber for the polarographic reduction of O_2 was bounded by a gas-permeable membrane based on a negative photoresist. The membrane provided for electrochemical stability within the device, protected the sensing surface from biofouling and controlled O_2 flux. However, such a Clark-type electrode construction, whilst having advantages for biointerfacing, does complicate micro-device construction and the scale-up of production. A commercially available medical system is marketed by Eppendorf. This microelectrode comprises a recessed gold/platinum wire combination in an insulating glass needle, in turn housed within a 300 μm outer diameter protective needle. The recessed gold surface is membrane protected, and so approximates to the desired structure for tissue measurements. Automated submillimetre advance and retraction within tissue allows multiple location measurements, but with post-retraction measurement obviating problems of tissue compression. Tama-Dasu *et al.* (2001) related the putative O_2 consumption of the electrode tip to simulated tissue measurements by differentially weighting O_2 at different three-dimensional locations in tissue. They concluded that, for limited measuring times, O_2 transport from more distant locations will be restricted, and so what the electrode provides is an 'averaged' approximation of the time value of clinical validity, which is not appropriate for data input into more formal tissue modelling procedures. In contrast, direct, free quantitative consumption of O_2 by a large electrode applied to the liver surface (Ag working electrode diameter 3 mm) was used intentionally by Seifalian *et al.* (2000) to measure perfusion driven delivery of O_2 to the liver. The electrode had a highly permeable covering membrane. Such a construction could, perhaps, provide a measure of cutaneous circulatory changes.

However, for skin non-invasive monitoring, the conventional approach has been that of the heated transcutaneous pO_2 electrode (Huch & Huch 1976). Here, heating permeabilizes the thick outer stratum corneuin of skin to allow rapid O_2 diffusion. The route taken involves numerous biological barriers, but heating stabilizes and also arterializes the dermal capillary bed. Whilst accuracy is compromised in relation to thicker adult versus neonatal skin, where the electrode has seen most application, Stücker *et al.* (2000*a*) used such an electrode to measure O_2 consumption by skin in patients with chronic venous skin lesions. They measured transcutaneous skin pO_2 reduction after arresting

arterial O_2 supply and, using the pO_2 solubility coefficient for skin, were then able to determine skin O_2 consumption, and differences for patients with and without venous ulceration. Evident lowering of transcutaneous pO_2 was judged to be a late onset phenomenon.

A more distributive assessment of tissue oxygen, short of a three-dimensional O_2 map, is to create a pO_2 distribution profile. Using the Eppendorf short penetration/retraction procedure, Nozue *et al.* (1997) undertook a thorough evaluation of pO_2 distribution in defined tumour volumes. There was semi-quantitative agreement between laboratories of the population of tumour hypoxic zones, and such a methodology could also enable more quantitative assessment of skin hypoxia.

3. FIBRE-OPTIC O_2 SENSORS

Optically based O_2 sensors almost all exploit the interference of O_2 on the quantum yield and/or lifetime of excited fluorescent or phosphorescent molecules. Specially formulated dyes with high-efficiency O_2 quenching have allowed for the fabrication of miniaturized fibre-optic probes able to monitor pO_2 over the medically important range (Wolfbeis 1991). The reversible, dynamic quenching occurs through the formation of an oxygen charge-transfer complex on collision of O_2 with the excited fluorophor, which in turn leads to non-radiative transfer to the ground state. For the purposes of invasive, transcutaneous monitoring, it is optimum to attach the reagent to the fibre-optic tip. The fibre-optic probe of Peterson & Vurek (1984) translated the principle of O_2 quenched fluorescence of a dye to a practical solution (figure 2). The advantage of this approach is that the electrode truly approaches equilibrium, and so does not consume O_2 as such; there is no dependence on external tissue flux, and so the device is independent of sample properties. Moreover, there is no external electrical interference. A simple probe without need for a reference electrode (unlike electrochemical devices) is usable. The flexibility of fibre-optics is certainly a disadvantage with respect to implantation, but if, for example, a narrow needle (figure 2) or indeed a retractable needle is used, then direct insertion is possible. The remaining device is a tissue compliant, flexible probe that is less liable to induce pain, tissue irritation or ongoing trauma.

There is now interest in the development of microscale optical probes, e.g. tip diameters in the range 10–30 µm. To further create compact systems, the O_2 quenched indicator is required to be addressable by a light emitting diode (LED) and a luminescent lifetime of greater than 1 µs is regarded as appropriate (Klimant *et al.* 1997). Ruthenium (II) tris(dipyridye) type organometallic complexes have proved attractive for this reason; they can have fluorescence lifetimes of up to 5.0 µs, i.e. efficiently quenched by oxygen, excitation wavelengths (approximately 460 nm) suited to blue LEDs and demonstrate large Stokes shifts (emission maxima ~600 nm). Variants on the organometallic model include ruthenium and platinum phosphorescent complexes with porphyrins, which have proved

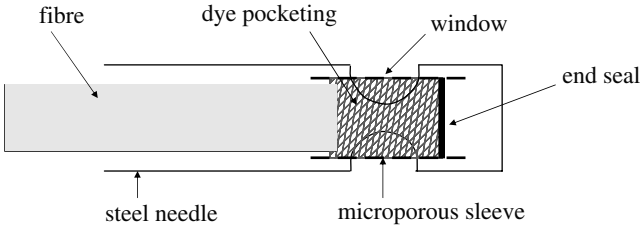

Figure 2. Fibre-optic O_2 sensor based on dye fluorescence quenching exploitation of microporous membrane to retain perylene dibutyrate dye (after Stefansson *et al.* 1989).

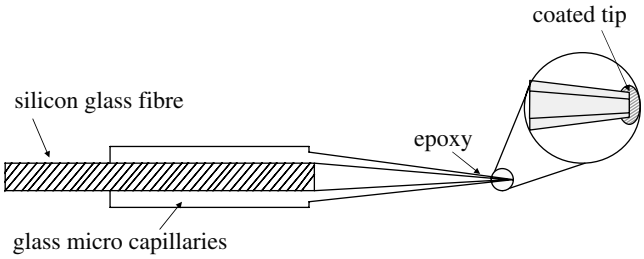

Figure 3. Oxygen microelectrode based on a tapered silica-glass fibre fixed in a glass microcapillary (after Holst *et al.* 1997).

attractive for microlectrodes because of strong phosphorescene, the ease of polymer matrix entrapment and high phosphorescence yields (Papkovsky *et al.* 1991).

For microelectrode fabrication, the simple basic rules (Klimant *et al.* 1997) are that high indicator activity per unit area is required, there needs to be good mechanical integrity with strong adherence to the optical interface and a higher degree of rigidity of the immobilizing matrices than for conventional, larger electrodes (namely PMMA, sol gels). With optimization of the retaining polymer matrix, it is possible to create multi-element arrays (Gauglitz & Brecht 1997) not only for topological and spatial resolution, but to permit more sophisticated multivariate analysis for self correction and measurement verification during use. Conversion to a practical structure was reported by Holst *et al.* (1997) who formed multiple flame-tapered optode tips of 20–30 µm (figure 3) and a retained indicator within a polystyrene matrix. They used the reduced lifetime of the luminescence to determine O_2 quenching, thereby avoiding the effects of dye photobleaching, optical background, sample optical properties and the complicating effects of add-on optical insulation. The operational set-up utilized sinusoidal light excitation; dye lifetime decay induced a phase delay in emitted light. Phase angle shift allowed the measurement of O_2 flux at the forearm skin surface from atmospheric air using a planar dye-loaded sensor foil (Holst *et al.* 1995). In these studies, cuff inflation to occlude local circulation led to a drop in superficial skin pO_2 and therefore increased air-skin pO_2 gradients, facilitating pO_2 uptake from the ambient air. Andrezejewski *et al.* (2002) simplified the task of microsecond light decay processing by measuring signal amplitudes at two distinct frequencies for differentiated

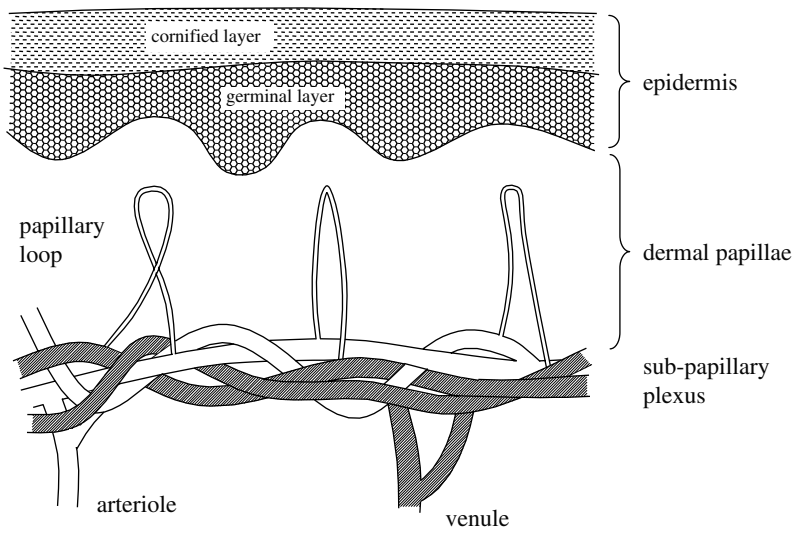

Figure 4. Diagrammatic representation of the outer layers of human skin consisting of dermal papillae and epidermis. The sub-papillary plexus gives rise to a single papillary loop in each dermal papilla. Cells in the epidermis undergo maturation from the germinal layer adjacent to dermal papillae to the stratum corneum in the outmost layer that is shed continuously.

light modulation readily followed by lock-in amplifiers instead of high-speed photodetectors.

For long-term monitoring, photobleaching is a concern, with evidence that, as well as the expected decrease in emission intensity, decay time may also be affected. Hartmann *et al.* (1997) monitored the contributory effects of singlet oxygen (generated by quenching) on the photobleaching process, and were able to mitigate these through co-incorporation of amine singlet oxygen scavengers.

The principle of fluorescence lifetime decay has been used for skin surface pO_2 imaging, on the basis that multiple electrode arrays cannot provide equivalent spatial resolution. Hartmann *et al.* (1997) developed ruthenium (II) organometallic based O_2 permeable films, and topographical lifetime images were obtained that related to spatial O_2 distribution on a submillimetre scale using a CCD camera. Transparent planar O_2 sensors for such imaging have been developed by Holst & Grunwald (2001), who embedded ruthenium (II)-tris-4, 7-diphenyl-1, 10-phenanthroline with trimethylsilypropanesulphonate as counter ion in PVC coated over transparent polyester. The advantage of the transparent construction is that pO_2 distribution can be correlated directly with structural images.

Future optical sensors will have greater stability and biocompatibility. However, improvements in optical characteristics such as excitation/emission maxima, indicator stability, quantum yield and decay profile are likely with new indicators and better polymeric immobilization strategies (Papkovski 1995).

4. CUTANEOUS MICROCIRCULATION

The cutaneous microcirculation has a unique anatomical arrangement that accommodates different and sometimes conflicting functions—the supply of nutrients, clearance of waste products and control of heat exchange (Wheater *et al.* 1979). The arterial supply and venous drainage to the skin are located deep in the hypodermis. They give rise to arterioles and venules to form two important plexuses in the dermis: the deeper cutaneous plexus at the junction of the hypodermis and the dermis and the superficial sub-papillary plexus just beneath dermal papillae (Braverman 1997). The sub-papillary plexus supplies the upper layer of the dermis and gives rise to a capillary loop in each dermal papilla. In the epidermis, cells produced by mitosis in the germinal layer undergo different stages of maturation and move progressively to the outer layers. The cornified layer in the outer most region of the skin consists of flattened cell remnants that are constantly shed (figure 4).

The superficial layer of the skin is the region between the sub-papillary plexus and the surface of the skin. While there is recent evidence that O_2 entering the skin from the atmosphere may meet the oxygen requirements of the cells in these areas (Stücker *et al.* 2002*a*), countercurrent arranged capillary loops in the papilla and their significance to oxygen delivery to the epidermis has not be investigated (Wang *et al.* 1996; Wang 2000). While there have been many studies on mechanisms of oxygen transport within tissues including the skin (see the reviews by Scheuplein & Blank (1971), Popel (1989) & Pittman (1995)), much of the experimental work on skin has been limited to estimates of mean tissue pO_2 from measurements of transcutaneous pO_2 or has used needle electrodes that were large relative to the dermal papilla (e.g. Evans & Naylor 1966; Spence & Walker 1976; Lübbers 1987; Opitz & Lübbers 1987; Jaszczak 1991; Harrison *et al.* 2002). There have been few attempts to relate the spatial distribution of pO_2 to the arrangement of the cutaneous microcirculation using small oxygen sensitive microelectrodes (Wang *et al.* 2003).

5. MICROELECTRODES FOR pO_2 IN HUMAN SKIN

In studies using small microelectrodes, pO_2 measurements are limited to the superficial layers of the skin,

since the penetration of deeper skin and underlying muscle requires much stronger, hence bigger electrodes. Oxygen sensitive microelectrodes were made using platinum–iridium wire. A short length of 25 µm diameter Pt–Ir wire (Goodfellow, Cambridge) was electrochemically etched to a slender profile with a tip diameter of less than 1 µm in saturated nitric acid solution. It was soldered to a conducting wire and was then fixed inside a 1.5 mm standard-walled glass pipette (Clark, Reading) using epoxy resin Araldite (Winlove & O'Hare 1993). The glass pipette was mounted on a micropipette puller (Narishige, Japan), which pulled the electrode to the desired tip size and profile. The pulling conditions were adjusted so that the glass sealed around the top of the wire. The tip of the electrode was bevelled using a micropipette grinder (Narishige, Japan) to enable easy tissue penetration. The tip of the finished electrodes was approximately 3–8 µm in diameter, giving a theoretical spatial resolution of 20–50 µm. The surface of the metal electrodes was cleaned by sonication in distilled deionized water and was coated with Nafion perfluorinated ion exchange resin (Sigma–Aldrich, Dorset).

To investigate the effects of occluding the local microcirculation on the tissue pO_2, some electrodes were made with special ϕ-shaped tips by repeated heating of the tip of the pulled electrode using the heating element of the micropipette puller and fusing a small glass bead to the shaft approximately 200 µm above the tip. These microelectrodes behaved identically to conventional electrodes as they penetrated the tissue up to the depth at which the bulbous region of the glass shield came into contact with the skin surface. Further advance of the electrode now compressed the underlying tissue, occluding the local microcirculation. This provided a convenient method for investigating the transient effects of microcirculatory arrest upon tissue pO_2.

All electrodes were tested for their electrochemical characteristics and were kept in saline for storage before and after testing and measurements. Calibration of electrodes was carried out before and after each experiment in saline bubbled with 100% N_2, air and 97% O_2 + 3% CO_2 to provide pO_2 values at atmospheric pressure. It is not uncommon for electrodes of this size to break during experiments. The most common cause of these accidents was unconscious movements of the finger during experiments. Penetration of skin and advance of electrodes in tissue were also occasionally responsible. If an electrode broke while in the tissue, the area was viewed under the microscope and any broken remnants of electrode were removed. The stratum corneum was removed for easier electrode penetration using adhesive tape before the start of an experiment. The lower arm and hand of the subject were taped on to a steel plate on the table to minimize excessive movement of the hand. The reference electrode (Ag/AgCl ECG electrode) was placed on the skin near the finger. The microelectrode was mounted on a three-dimensional remote hydraulic micromanipulator (Narishige, Japan), which in turn was mounted on a three-axial coarse micromanipulator (Narishige, Japan). Both the working and reference electrodes were connected to the potentiostat (CV37, BAS). Currents from the potentiostat at −0.75 V versus Ag/AgCl were recorded on a chart recorder.

Skin was illuminated using a cool light source. Paraffin oil was superfused over the finger to minimize the transport of oxygen from the air and to reduce light reflections from the surface of the skin. A Wild M10 stereomicroscope (Leica) was used to visualize nail fold capillaries and flows in these capillaries. No measurements of blood-flow velocity were made, but red cells were used as markers to indicate flow conditions (e.g. flow stopped, partially stopped, reinstated). The coarse micromanipulator was used to position an electrode just above the site of the measurement, while the remote hydraulic micromanipulator was used for the penetration of the skin and movement of the electrode within the tissue.

In all measurements, the oxygen partial pressure of the air is 160 mmHg at sea level and at room temperature.

6. SPATIAL VARIATIONS OF pO_2 IN SUPERFACIAL LAYERS OF SKIN

Mean values for the spatial variations of the pO_2 with depth in the outer skin are presented in figure 5. In figure 5*a*, mean pO_2 (±SD) has been plotted for the superficial (5–10 µm), the middle (45–65 µm) and deep (100–120 µm) regions in the dermal papilla of finger nail folds. It is seen that the pO_2 increases with depth from the surface of the skin to the dermis. With paraffin oil applied on top of the nail fold, pO_2 was lowest at the surface of the skin. In the superficial region of the skin, pO_2 is approximately 8.0 ± 3.2 mmHg ($n = 6$). The value increases to 24.0 ± 6.4 mmHg ($n = 8$) in dermal papillae, and at the depth just above the sub-papillary plexus, pO_2 is approximately 35.2 ± 8.0 mmHg ($n = 9$). Student's t-test showed that these results differed very significantly: between the superficial and the middle regions to a level of $p < 0.000\,05$, and between the middle and the deep regions to a level of $p < 0.005$.

pO_2 along the axis of papillary loops was measured, mean pO_2 (±SD). These measurements were carried out with the microelectrode tip at points in the tissue that were close to the most distal (and hence most horizontal) capillary loops of the nail fold. As shown in figure 5*b*, pO_2 generally decreased from the base to the tip of the papillary loop. At the base of the loop, pO_2 is approximately 40 ± 4.8 mmHg ($n = 6$), the value drops to 35.2 ± 3.2 mmHg in the middle ($n = 6$) and approximately 30.4 ± 5.2 mmHg near the tip of the loop ($n = 6$). Student's t-test revealed that $p < 0.01$ between data at the base and the tip of the papillary loop; however, the differences between values at the base and the middle of the papillary loop or between the middle and the tip of the loop are not significant (i.e. $p < 0.13$ and $p < 0.10$, respectively).

7. TEMPORAL VARIATIONS OF pO_2 FOLLOWING MICRO-OCCLUSION

Tissue oxygen content is the balance between the oxygen supply and oxygen consumption. To gain insight into this, special ϕ-shaped electrodes were used to

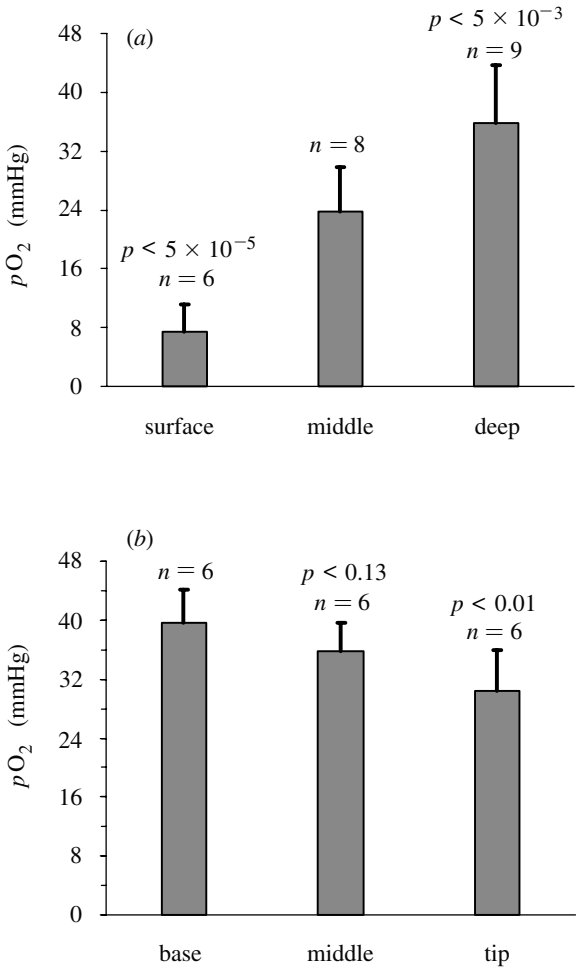

Figure 5. Spatial variations of pO_2 in the outer layers of the nail fold skin (from Wang *et al.* 2003). (*a*) Mean values for pO_2 at depths of 5–10 µm (surface), 45–65 µm (middle) and 100–120 µm (deep) in all areas of the nail fold skin. The pO_2 at the surface and in the deep regions differ very significantly from those in the middle region ($p < 0.000\,05$ and $p < 0.005$, respectively). (*b*) Mean values for pO_2 with depth in tissue close to the axis of the capillary loops of the papillae. While pO_2 at the tip differs significantly from its value at the base ($p < 0.01$), the gradient is too small for significant differences to be detected between the pO_2 of the tissues around the middle of the capillary loops and the pO_2 at the tip and the base.

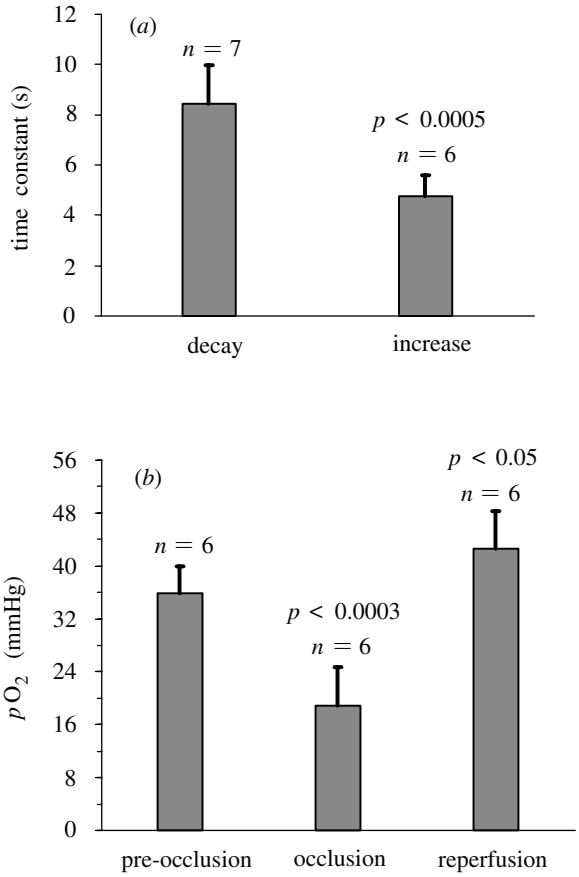

Figure 6. Temporal characteristics in localized microvessel occlusion and reperfusion (from Wang *et al.* 2003). (*a*) Time constants of mono-exponential decays of the pO_2 during microvessel occlusion differed significantly to those of exponential rises in reperfusion ($p < 0.0005$). (*b*) Mean values for pO_2 before, during and after local reduction in blood flow. After reduction in blood flow, mean pO_2 was very significantly reduced ($p < 0.003$). After restoration of flow, pO_2 was increased to levels significantly above the initial control values ($p < 0.05$).

investigate the transient changes in skin pO_2 when the microcirculation is suddenly arrested and restored.

In experiments where flow in the capillary and underlying sub-papillary plexus was either reduced or stopped, pO_2 in dermis decreased with the time in all cases by 16–24 mmHg. New steady values in pO_2 were reached within 30–60 seconds following alterations in capillary flow. The dynamic changes in pO_2 with the time can be described by a single exponential decay function,

$$P = a\exp(-t/\tau) + b,$$

where P is the value of the pO_2 during the transient, τ is the time constant, a represents the difference between the initial and final values of pO_2 and b is the final value of pO_2.

After a period of microcirculatory arrest lasting between 1 and 5 minutes, flow was restored. The increase in pO_2 can be described by a similar single exponential function,

$$P = a'[1 - \exp(-t/\tau')] + b',$$

with τ' being the time constant for the exponential rise, and a' and b' representing the range and initial value of pO_2.

Time constants (mean ± SD) for the exponential decays (ischaemia) and rises (reperfusion) of the pO_2 are shown in figure 6*a*. It was found that the mean time constant for decays, $\tau = 8.44 \pm 1.53$ s ($n = 7$), is consistently greater than that for the exponential rises, $\tau' = 4.75 \pm 0.82$ s ($n = 6$). A two-tailed t-test was applied to the data and revealed a significant difference between the time constants ($p < 0.0005$).

In figure 6*b*, steady values of the pO_2 (mean ± SD) following ischaemia and after reperfusion were compared with their values prior to arrest of the microcirculation (the control state). There is a significant decrease

in the pO_2 following arrest of the local microcirculation. pO_2 falls from a mean of 35.2 ± 4.8 mmHg ($n = 6$) to 19.2 ± 6.4 mmHg ($n = 6$), i.e. a fall in pO_2 of 16 mmHg. The non-zero value for pO_2 following tissue compression is caused by either the partial occlusion of the circulation in some experiments or O_2 supply from neighbouring vessels or both. When blood flow is restored pO_2 increases to 43.2 ± 6.4 mmHg ($n = 6$), an increase of approximately 125% in comparison with the value in ischaemia. This value, interestingly, is also 23% greater than the control. Student's *t*-test revealed that differences in pO_2 between ischaemia and control, or between ischaemia and reperfusion were highly significant ($p < 0.0003$ and $p < 0.000\,04$, respectively). There was also significant difference between pO_2 values in control and in reperfusion, $p < 0.05$.

8. O_2 SUPPLY TO SKIN

The study using small microelectrodes showed that when the skin of the human finger nail fold is covered with paraffin oil, the pO_2 in the tissue increases with depth from values close to zero at the surface to about 40–50 mmHg close to the sub-papillary plexus. These agree with previous experimental and theoretical estimates of pO_2 in this part of the skin (e.g. Grossmann 1982; Jaszczak, 1991; Baumgärtl *et al.* 1987; Stücker *et al.* 2000*b*). The observation that pO_2 increases with depth would be predicted if all O_2 is delivered to the papillary dermis and epidermis from the sub-papillary plexus. Under physiological conditions, however, O_2 can enter the outermost layers of the skin from the atmosphere and recent measurements of Stücker *et al.* (2002) have shown this may be as much as 5.3 ml cm^{-2} min^{-1} and would be sufficient to meet the needs of the epidermis. Under these conditions the pO_2 profile with depth beneath the skin surface might be expected to differ considerably from that reported by Wang *et al.* (2003). Although there is now strong evidence that O_2 may enter the skin from the atmosphere, the study by Wang *et al.* (2003) demonstrated that when this is prevented, the oxygen supply to the epidermis and superficial dermis can be maintained by the papillary microcirculation. There is also a suggestion that the papillary microcirculation is regulated to meet the O_2 requirements of the tissue at a very local level.

9. EFFECTS OF LOCALIZED ISCHAEMIA REPERFUSION

The exponential decline in pO_2 when flow is stopped is most likely to be caused by consumption of the oxygen in tissue and the blood, and would be consistent with the discharge of O_2 from stores in the tissue. The most likely site of these O_2 stores is the haemoglobin of the red cells in the capillaries where flow has been arrested. The oxyhaemoglobin dissociation curve is approximately linear over the range of pO_2 between 40 and 15 mmHg, and the unloading of O_2 over this range might be expected to approximate to a single exponential function.

The rise of pO_2 to a new steady state as flow is restored is determined by the rate at which the pO_2 in capillaries is returned to their pre-occlusion values. This is primarily dependent on the blood flow velocity in the re-perfused capillaries. If the tissue at the tip of the microelectrode is principally supplied by O_2 from a point along a nearby capillary, the rate at which capillary pO_2 will rise at this point will depend on how rapidly blood with a higher pO_2 reaches that point and how much the blood pO_2 falls between leaving the arteries and arriving at this point. Provided that the O_2 consumption of the tissue remains constant, the extraction (i.e. the O_2 lost from unit volume of blood) should be largely dependent on the blood flow. If the post-occlusion flow is greater than in the pre-occlusion state, not only will the pO_2 rise rapidly, but it should rise to a higher level than it was initially. The tissue pO_2 should then remain above its initial value for as long as the flow is elevated. This is just what has been observed. When blood flow is restored, tissue pO_2 rises to a value that is 23% higher than its pre-occlusion value. This is consistent with either a decrease in tissue O_2 consumption or a significant degree of reactive hyperaemia. Assuming that tissue O_2 consumption is the same as in the pre-occlusion state, the 23% increase in pO_2 is equivalent to an increase in O_2 saturation in the blood of the nearest capillaries from 70 to 85%. If the saturation of the arterial blood is 95%, the increase in blood flow equivalent to the rise in tissue pO_2 is of the order of 2.5-fold. This calculation indicates that reactive hyperaemia occurs with a high spatial resolution in skin and this would be consistent with the very localized hyperaemic responses seen in some other tissues (Burton & Johnson 1972). Although the rise in pO_2 accompanying reperfusion can be described approximately by a single exponential, the data are less regular than those describing the decline on pO_2 with vascular occlusion. This may represent fluctuations in blood-flow velocity or red cell flux with the restoration in flow (Johnson & Wayland 1967).

10. FUTURE PROSPECTS

The electrochemical and fibre-optic devices described in this section are best regarded as semi-implantable and minimally invasive. They have the potential to provide localized information of (at least) approximate pO_2 in pre-specified skin and skin ulcer microenvironments. There are two major developments that are likely to improve spatial discrimination and reliability. First, evolving microfabrication techniques will allow robust probe structures to be fabricated as arrays able to penetrate in and around the ulcer wound site, but with negligible local trauma. This 'atraumatic' insertion should minimize local tissue reaction with less tissue disruption. Devices will then become truly minimally invasive and yet have a high sensor/interrogation density, almost with the features of a chemically reactive velcro. A further advantage will be of a high level of sensor redundancy, allowing for greater confidence in the measurements. With appropriate additional hollow microneedle and microinjection capability along such arrays, it could be envisaged that pharmacologically active agents might be injected locally, e.g. vasodilators to monitor the reactivity of localized circulation as

a possible dynamic indicator of tissue integrity. The second key advance will come from materials science. Membrane technology has already improved the stability and biocompatibility of biosensors. Further advances should help to reduce the inevitable drift that O_2 sensors suffer due to surface fouling and contamination (Reddy & Vadgama 1997).

Other possible advances will exploit skin ulcer tissue embedded optical nanoprobes coated with, say, O_2 reactive dyes, so developing the recent concept of probes encapsulated by biologically localized embedding, so called PEBBLE sensors (Xu *et al.* 2001). Whilst such micron scale spheroids have allowed distributed sensing *in vitro*, the correct formulation may enable safe *in vivo* use and, moreover, with near-infrared active dyes, interrogation of deeper skin layers becomes possible. The ultimate goal must be sensor-based feedback on a real-time basis so that local pO_2, a key surrogate of tissue metabolic status, can be used to optimize pressure ulcer therapeutic regimens.

The authors wish to thank Monika Scheonleber for her help with this manuscript.

REFERENCES

Andrzejewski, D., Klimant, I. & Podrielska, H. 2002 Method of lifetime-based chemical sensing using the demodulation of the luminescence signal. *Sensors Actuators* B **84**, 160–166.

Baumgärtl, H., Ehrly, A. M., Saeger-Lorenz, K. & Lubbers, D. W. 1987 Initial results of intracutaneous measurement of PO_2 profiles. In *Clinical oxygen pressure measurement* (ed. A. M. Ehrly, J. Hauss & R. Huch), pp. 121–128. Berlin: Springer.

Braverman, I. M. 1997 The cutaneous microcirculation: ultrastructure and microanatomical organization. *Microcirculation* **4**, 329–340.

Burton, K. S. & Johnson, P. C. 1972 Reactive hyperemia in individual capillaries of skeletal muscle. *Am. J. Physiol.* **223**, 517–524.

Clark, L. C. 1956 Monitor and control of blood and tissue oxygen tension. *Trans. Am. Soc. Internal Organs* **2**, 41–46.

Davies, P. W. & Brink, F. 1942 Microelectrodes for measuring local oxygen tension I animal tissues. *Rev. Sci. Instrum.* **13**, 524–533.

Evans, N. T. S. & Naylor, P. F. D. 1966 Steady states of oxygen tension in human dermis. *Respir. Physiol.* **2**, 46–60.

Gauglitz, G. & Brecht, A. 1997 Recent developments in optical transducers for chemical and biochemical applications. *Sensors Actuators* B **38**, 1–7.

Grossmann, U. 1982 Simulation of combined transfer of oxygen and heat through the skin using a capillary-loop model. *Math. Biosci.* **61**, 205–236.

Harrison, D., Lübbers, D., Baumgärtl, H., Stoerb, C., Rapp, S., Altmeyer, P. & Stücker, M. 2002 Capillary blood flow and cutaneous uptake of oxygen from the atmosphere. In *Functional monitoring and drug tissue interaction* (ed. M. D. Kessler & G. J. Mueller). Proceedings of SPIE, vol. 4623, pp. 195–205. Bellingham, WA: SPIE.

Hartmann, P., Ziegler, W., Holst, G. & Lübbers, D. W. 1997 Oxygen flux fluorescence lifetime imaging. *Sensors Actuators* B **38**, 110–115.

Holst, G. A., Köster, T., Voges, E. & Lübbers, D. W. 1995 Flox-on oxygen-flue-measuring system using a phase-modulation method to evaluate the oxygen-dependent fluorescence lifetime. *Sensors Actuators* B **29**, 231–239.

Holst, G., Glud, R. N., Kühl, M. & Klimant, I. 1997 A microoptode array for fine-scale measurement of oxygen distribution. *Sensors Actuators* B **38**, 122–129.

Holst, G. & Grunwald, B. 2001 Luminsecence lifetime imaging with transparent oxygen optodes. *Sensors Actuators* B **74**, 78–90.

Huch, A. & Huch, R. 1976 Transcutaneous, non-invasive monitoring of pO_2. *Hospital Practices* **6**, 43–52.

Jaszczak, P. 1991 Skin oxygen tension, skin oxygen consumption and skin blood flow measured by a tc-pO_2 electrode. *Acta. Physiol. Scand.* **143**, 53–57.

Jöbsis, F. F. 1977 Non invasive infrared monitoring of cerebral and myocardial oxygen insufficiency and circulatory parameters. *Science* **198**, 1264–1266.

Johnson, P. C. & Wayland, H. 1967 Regulation of blood flow in single capillaries. *Am. J. Physiol.* **212**, 1405–1415.

Klimant, I., Kühl, M., Glud, R. N. & Holst, G. 1997 Optical measurement of oxygen and temperature in microscale: strategies and biological applications. *Sensors Actuators* B **38**, 29–37.

Lübbers, D. W. 1987 Theory and development of transcutaneous oxygen pressure measurement. *Int. Anesthesiol. Clin.* **25**(3), 31–65.

McDonnell, M. B. & Vadgama, P. 1989 Membranes: separation principles and sensing. In *Selective electrode reviews* (ed. J. D. R. Thomas), vol. 11, pp. 17–67. Oxford: Pergamon Press.

Nozue, M. *et al.* 1997 Interlaboratories variation of oxygen tension measurement by Eppendorf 'Histograph' and comparison with hypoxic marker. *J. Surg. Oncol.* **66**, 30–38.

Opitz, N. & Lübbers, D. W. 1987 Theory and development of fluorescence-based optochemical oxygen sensors—oxygen optodes. *Int. Anesthesiol. Clin.* **25**(3), 177–197.

Papkovsky, D. P., Olah, J., Troyanovsky, I. V., Sadovsky, N. A., Rumyantseva, V. D., Mironov, A. F., Yaropolov, A. I. & Savitsky, A. P. 1991 Phosphorescent polymer films for optical oxygen sensors. *Biosensors Bioelectron.* **7**, 199–206.

Papkovsky, B. D. 1995 New oxygen sensors and their application to biosensors. *Sensors Actuators* B **29**, 213–218.

Peterson, J. J. & Vurek, G. G. 1984 Fibre-optic sensors for biomedical applications. *Science* **224**, 123.

Pittman, R. 1995 Influence of microvascular architecture on oxygen exchange in skeletal muscle. *Microcirculation* **2**, 1–18.

Popel, A. S. 1989 Theory of oxygen transport to tissue. *Crit. Rev. Biomed. Eng.* **17**, 257–321.

Reddy, S. M. & Vadgama, P. 1997 Membranes to improve amperometric sensor characteristics. In *Handbook of biosensors and electronic noses: medicine, food, and the environment* (ed. E. Kress-Rogers), pp. 111–135. Boca Raton, FL: CRC Press.

Scheuplein, R. J. & Blank, I. H. 1971 Permeability of the skin. *Physiol. Rev.* **51**(4), 702–747.

Schneiderman, G. & Goldstick, T. K. 1978 Oxygen electrode design criteria and performance characteristics recessed cathode. *J. Appl. Physiol.* **45**, 145–154.

Seifalian, A. M., Mallett, S., Piasecki, C., Rolles, K. & Davidson, B. R. 2000 Non-invasive measurement of hepatic oxygenation by an oxygen electrode in human orthotopic liver transplantation. *Med. Eng. Phys.* **22**, 371–377.

Silver, I. A. 1987 Microelectrodes in medicine. *Phil. Trans. R. Soc. Lond.* B **316**, 161–167.

Spence, V. A. & Walker, W. F. 1976 Measurement of oxygen tension in human skin. *Med. Biol. Eng.* **14**, 159–165.

Stefansson, E., Peterson, J. I. & Wang, Y. H. 1989 Intraocular oxygen tension measured with a fibre-optic sensor in normal and diabetic drugs. *Am. J. Physiol.* **256**, H1127–H1133.

Stücker, M., Falkenber, M., Reuthor, T., Altmeger, P. & Lübber, D. W. 2000*a* Local oxygen content in the skin is increased in chronic venous incompetence. *Microvascular Res.* **59**, 99–106.

Stücker, M., Altmeyer, P., Struk, A., Hoffmann, K., Schulze, L., Rochling, A. & Lübbers, D. W. 2000*b* The transepidermal oxygen flux from the environment is in balance with the capillary oxygen supply. *J. Invest. Dermatol.* **114**, 533–540.

Stücker, M., Struk, A., Altmeyer, P., Herde, M., Baumgärtl, H. & Lübbers, D. W. 2002 The cutaneous uptake of atmospheric oxygen contributes significantly to the oxygen supply of human dermis and epidermis. *J. Physiol.* **538**(3), 985–994.

Suzuki, H., Kojima, N., Sugame, A., Takei, F. & Ikegami, K. 1990 Disposable oxygen electrodes fabricated by semi conductor techniques and their application to biosensors. *Sensors Actuators* B **1**, 528–532.

van der Kleij, J. A. & de Koning, J. 1981 Tissue oxygen electrode for routine clinical application. In *Monitoring of vital parameters during extracorporeal circulation* (ed. H. P. Kimmich), pp. 95. Basel: Karger.

Tama-Dasu, I., Waites, A., Dasu, A. & Denekamp, J. 2001 Theoretical simulation of oxygen tension measurement in tissues using a microelectrode: I. The response function of the electrode. *Physiol. Meas.* **22**, 713–725.

Wang, W., Parker, K. H. & Michel, C. C. 1996 Theoretical studies of steady state transcapillary exchange in countercurrent systems. *Microcirculation* **3**, 301–311.

Wang, W. 2000 A critical parameter for transcapillary exchange of small solutes in countercurrent systems. *J. Biomech.* **33**, 433–441.

Wang, W., Winlove, C. P. & Michel, C. C. 2003 Oxygen partial pressure in outer layers of skin of human finger nail folds. *J. Physiol.* **549**(3), 855–863.

Whalen, W. J. & Spande, J. I. 1980 A hypodermic needle pO_2 electrode. *J. Appl. Physiol.* **48**, 186–187.

Wheater, P. R., Burkitt, H. G. & Daniels, V. G. 1979 *Functional histology*, pp. 116–127. New York: Churchill Livingstone.

Winlove, C. P. & O'Hare, D. 1993 Electrochemical method in physiology. *Current Topics Electrochem.* **2**, 345–361.

Wolfbeis, O. S. 1991 *Fiber optic chemical sensors and biosensors.* Boca Raton, FL: CRC Press.

Xu, H., Aylott, J. W., Kopelman, R., Miller, T. J. & Philbert, M. A. 2001 A real-time ratiometric method for the determination of molecular oxygen inside living cells using sol-gel based spherical optical nanosensors with applications to rat C6 glioma. *Anal. Chem.* **73**, 4124–4133.